Available online at www.sciencedirect.com

ScienceDirect

materialstoday: PROCEEDINGS

International symposium on Nanostructured, Nanoengineered and Advanced Materials, ISNNAM 2020

Evaluation of silica sodalite infused polysulfone mixed matrix membranes during H_2/CO_2 separation

C.L Eden[a], M.O. Daramola[b,*]

[a]*School of Chemical and Metallurgical Engineering, Faculty of Engineerinng and the Built Environment, University of the Witwatersrand, Wits 2050, Johannesburg, South Africa;*
[b]*Department of Chemical Engineering, Faculty of Engineering, Built Environment and Information Technology, University of Pretoria, Private bag X20 Hatfield, Pretoria 0028, South Africa*
**Corresponding author: mikkydara@gmail.com*

Abstract

Global warming and environmental degradation have stimulated the drive towards the capture of large point source carbon emissions and reducing high energy intensity of industrial processes. Mixed membranes infused with high porosity silica sodalite are potential useful for pre-combustion CO_2 capture. However, development of high quality mixed matrix membranes is a challenge. In this study, silica sodalite (SSOD) infused polysulfone (PSF) membranes were developed and evaluated for pre-combustion CO_2 capture. The SSOD was obtained via topotactic conversion of layered silicates; and the membrane was prepared using the phase inversion method. The physicochemical nature of the SSOD and the SSOD/PSF was checked using XRD, SEM, and N_2 physisorption at 77 K. Single gas permeation used to check membrane quality. N_2 physisorption shows that the SSOD possesses higher surface area of 56.56 m^2/g and pore volume of 0.181 cm^3/g, when compared to that of the hydrothermally-synthesized hydroxy sodalite (HSOD) crystals (surface area: 27.43 m^2/g; pore volume: 0.084 cm^3/g). The SSOD/PSF membrane is asymmetric with higher mechanical strength than the ordinary PSF. Loading the PSF with SSOD enhanced its H_2 permeance from 4.9×10^{-7} mol/m^2.s.Pa but with a decrease in H_2/CO_2 separation factor from 2.2 to 0.6. While the enhanced H_2 permeance is attributed to the enhanced porosity of the SSOD, the ideal selectivity is low but still within the values reported in literature. Increasing the SSOD loading up to 10 wt. % enhanced the quality and performance of the PSF membrane, displaying H_2 permeance of 6.5×10^{-7} mol/m^2.s.Pa and a separation factor of 1.1. Though results reported in this study are promising, a robust synthesis protocol that will further enhance both the H_2 selectivity and H_2 permeance of the membrane is required. Furthermore, more studies are required on the process optimization and techno-economic feasibility for pre-combustion CO_2 capture.

Keywords: silica sodalite; mixed matrix membranes; pre-combustion; carbon capture

1. Introduction

Rapid environmental change and global warming associated with increasing levels of anthropogenic carbon dioxide have seen a global push towards carbon capture and the high energy efficiency of industrial processes. In addition, the increasing energy demand associated with urbanization and industrialization in developing countries such as South Africa, exacerbates the environmental situation [1]. The majority of South Africa's power production comes from the combustion of fossil fuels, carbon capture from large point source emitters such as power plants is

vital for sustainable energy generation. Pre-combustion carbon capture is favourable over post-combustion methods due to the higher CO_2 concentration (>20%) and pressure in the H_2/CO_2 flue gas [2]. Integrated gasification combined cycle (IGCC) power plants generate synthesis gas through the gasification process by heating carbon based fuels, such as coal, with air or oxygen. To produce more H_2, the carbon monoxide produced is then converted to hydrogen and carbon dioxide via the water-gas shift reaction (WGR) [3]. To separate the produced H_2 from the gas mixture; traditional separation technologies such as solvent adsorption and cryogenic distillation have been very efficient, but these methods are highly energy intensive or make use of environmentally damaging chemicals such as nitrosamines, nitramines and their degradation products [4, 5, 6]. However, the use of membrane systems is an alternative technology characterized with consistently high flux and selectivity, low energy intensity and simple operation [7]. Therefore, membrane systems could be employed in IGCC processes to either separate H_2 from the H_2/CO_2 mixture after the WGS reaction or be incorporated into the shift reactor to enhance the production of H_2 [8].

The majority of the membrane systems utilized industrially are polymeric based, polymers offer advantages over ceramic and non-polymeric membranes due to their inexpensive nature, ease of fabrication and good mechanical strength [9, 10, 11]. If the separation performance of polymer membranes can successfully be improved to exceed the permeability/ selectivity trade-off [12, 13], these membranes have the potential to compete with the high separation efficiency produced by traditional separation technologies. Glassy polymers have a good size-sieving ability promoting high selectivity in gas separation applications. Polysulfone (PSF) is a glassy polymer widely use in membrane applications with good mechanical, thermal and oxidative stability that can easily be fabricated on a large scale [14]. However, polymeric membranes could not be used in IGCC, especially in the WGS where the temperature could be above 200ºC. Ceramic membranes are more preferred in this situation, but they are fragile with high cost of production when compared to producing polymeric membranes [15, 16]. Utilizing mixed matrix membranes (MMMs) such as PSF filled with high porosity zeolite nanoparticles produces membranes that are not only thermally and mechanically stable but have the potential to improve separation performance of polymeric membranes by combining the selective nature of the PSF with that of the enhanced transport properties and size selective nature of the zeolite [17, 18].

One such zeolite is hydroxy sodalite (HSOD) that possesses cage structures and small pore apertures of 2.6Å enabling the separation of small molecules such as hydrogen (kinetic diameter of 2.89 Å) and water (kinetic diameter of 2.65Å) from larger molecules such as N_2 (kinetic diameters of 3.64 Å), O_2 (kinetic diameter of 3.46 Å), and CO_2 (kinetic diameter of 3.3Å) [19]. However, traditional hydrothermal synthesis of HSOD produces HSOD crystals with organic matter such as structural directing agents, water and anions trapped within the cage structures reducing their porosity for gas permeation [20]. Attempting to remove these occluded matters via dehydration (>400ºC) collapses the cage structures, and thus decomposes the material to other non-useful materials for gas separation [21, 15, 22]. However, topotactic conversion is a relatively new synthesis process that is able to produce higher porosity silica sodalite (SSOD), without the presence of occluded matter, through the conversion of RUB-15 silicate layers [23, 24, 25]. It is interesting to know that limited research is available in literature on the exploration of this method to develop SSOD employable in mixed matrix membranes for H_2/CO_2 separation applications [26, 27, 28]. In particular, sodalite infused mixed matrix composite membranes are relatively novel especially in H_2/CO_2 separation for potential pre-combustion applications. Against this background, this study investigated the synthesis and evaluation of SSOD infused PSF membranes for H_2/CO_2 separation. Within the study, attempt was made to investigate the effect of SSOD loading on the quality and separation performance of the membrane.

2. Experimental

2.1. Materials

Tetra-ethoxysilane (TEOS, reagent grade 98%, Sigma-Aldrich, South Africa), tetrametyl ammonium hydroxide (TMAOH, 25 wt. % in water, Sigma-Aldrich, South Africa) and acetone (Sigma-Aldrich, South Africa) were used as received for the synthesis of RUB-15. Propionic acid (>99.5 wt. %, Sigma Aldrich, South Africa) was used without purification for the production of the silica sodalite. Sodium metasilicate (Sigma-Aldrich, South Africa), sodium hydroxide pellets (Sigma-Aldrich, South Africa) and anhydrous sodium aluminate (Sigma-Aldrich, South Africa) was used for the production of hydroxy sodalite (HSOD) for comparison. Polysulfone (beads (transparent), Sigma-Aldrich, South Africa) and N,N-Dimethylacetamide (>99.9%, Sigma-Aldrich, South Africa) were used for

the fabrication of membranes. Nitrogen hydrogen, carbon dioxide and H_2/CO_2 (60:40) mixture gas cylinders were purchased from Afrox, South Africa with the corresponding gas regulators.

2.2. Synthesis and fabrication procedures

2.2.1 Particle synthesis

Silica sodalite (SSOD) was produced following the modified basic procedure of Moteki et al [24]. To prepare RUB-15, TEOS and TMAOH were combined in a 1:1 molar ratio and magnetically stirred for 24 hours in a PTFE cup. The solution was placed in a Teflon lines autoclave and heated at 140℃ for 7 days. The as-produced RUB-15 was washed with acetone, centrifuged and dried overnight in an oven at 60℃. The dried RUB-15 was crushed to yield a fine white powder. To convert the as-produced RUB-15 to SSOD, 0.1g was added to 30 ml of propionic acid (5M) and stirred for 3 hours at 900 rpm. The suspension was separated by centrifugation and repeatedly washed with deionized water. The resulted particles were then dried overnight in an oven at 60℃, and then calcined for 1 hour at 600℃. Hydroxy sodalite (HSOD) was synthesized following the procedure by Daramola et al [21, 29] for comparison. The resulted crystals were washed with deionized water and dried overnight in an oven at 100℃ [29].

2.2.2 Membrane fabrication

Mixed matrix membranes were produced through a wet phase inversion process. Measured amounts of SSOD (0, 5, 10, 15 wt. %) and HSOD (5 wt. %) were mixed with 20 ml of solvent (N,N Dimethylacetamide) and magnetically stirred for 3 hours before the addition of 5 g PSF. The mixture was stirred for 24 hours to dissolve the PSF. The solution was repeatedly ultra-sonicated for 30 minutes and stirred to ensure formation of homogeneous casting solution. The solution was stirred slowly and left for 5 minutes to expel the gas bubbles present within the casting solution. The solution was cast onto a glass plate using a "doctor blade" and immediately submersed in a bath of deionized water. The membrane was soaked for 24 hours in deionized water to ensure complete solvent removal, and oven dried at 60℃ for 2 hours [18].

2.3. Characterization

Single point Brunauer-Emmett-Teller (BET) analysis was conducted, from the results of Nitrogen physisorption at 77 K, to determine the surface area and pore volume of the as-produced sodalite particles. Powder X-ray diffraction (XRD) patterns were performed on the SSOD and HSOD using a Bruker D2 XRD with CuKα radiation (λ = 1.5406 Å) to analyze the crystalline and amorphous nature of the sodalite. Scanning electron microscopy (SEM) was conducted on a Carl Zeiss sigma field emission scanning electron microscope equipped with Oxford X-act EDS detector to examine the surface and cross-sectional morphology the samples. Fourier-transmission infrared spectroscopy (FTIR) was conducted on a PerkinElmer UATR two FT-IR spectrum two spectrometer to identify functional groups and the presence of occluded water. Thermogravimetric (TG) analysis was performed using AS Advanced laboratory solutions (Q600 SDT) with air as the carrier gas at a temperature ramp of 20℃/min up to a temperature of 900℃. Tensile strength analysis was conducted using a Stable Micro Systems texture analyser (TA-XT Plus) and Young's modulus calculations in order to assess the mechanical strength of the fabricated membranes. Membrane thickness was measured with an InSize digital outside micrometre (3109-25A) and utilized in gas permeability calculations. A custom-made gas separation rig, with a membrane module, was utilized for membrane gas separation and a pre-calibrated gas chromatography equipped with a TCD was used to analyse the gas feed, permeate and the retentate during the separation. Gas permeability, a function of sorption and diffusion coefficients (Equation 1) which are controlled by the membrane physical and chemical properties as well as those of the gas permeant and the interaction between the two, was obtained using Equation (2) [26]. The ideal selectivity (α) of gas a over gas b was obtained with the use of Equation (3) [7, 30]:

$$P_a = S_a D_a \tag{1}$$

$$P_a = \frac{l\,Q}{A\,\Delta p}\,\frac{273.15}{T} \tag{2}$$

$$\alpha_{a/b} = \frac{Pa}{Pb} \tag{3}$$

Where volumetric flowrate (Q), membrane thickness (l), membrane area (A) and transmembrane pressure drop (Δp), and ambient temperature (T) were measured and recorded from the separation rig using the in-built pressure monitor and controller.
The component permeability and selectivity during the mixture gas separation were obtained using Equation (5) and Equation (6), respectively. The gas mole fraction (x) in the permeate and the feed were determined through GC analysis using a response factor (Equation 4) from known concentrations.

$$x_{a,perm} = \frac{Peak\ area\ (uV..\min)}{Response\ factor_a} \tag{4}$$

$$Pi = \frac{X_{perm}\, l\, Q}{A\,(p_{feed}\, X_{feed} - p_{perm}\, X_{perm})} \tag{5}$$

$$\alpha_{a/b} = \frac{X_{perm,a}\,(p_{feed}\, X_{feed} - p_{perm}\, X_{perm})b}{X_{perm,b}\,(p_{feed}\, X_{feed} - p_{perm}\, X_{perm})a} \tag{6}$$

3. Results and discussion

3.1. Sodalite characterization

The BET surface area and the pore volume of the as-prepared HSOD were 27.43 m^2/g and 0.084 cm^3/g, respectively, while the BET surface area and the pore volume of the SSOD were 56.56 m^2/g and 0.181 cm^3/g, respectively. More than 100% increase in the BET surface area and an increase of about 116% in the pore volume were obtained for SSOD when compared to those from HSOD, indicating the efficiency of the topotactic synthesis method in removing the occluded matter from HSOD. The enhanced porosity of the silica sodalite should facilitate higher permeation of gas molecules through the sodalite cages [31], thereby potentially leading to improved gas transport and separation performance. Furthermore, the multipoint adsorption isotherms obtained for the SSOD (though not shown in this article) show that adsorption of SSOD is a Type 4 isotherm with an H4 hysteresis loop that characterizes mesoporous plate-like particles with slit pores [32].

The XRD patterns of the SSOD and HSOD (Fig. 1.A) are similar to the simulated XRD pattern of hydroxy sodalite crystals documented in the database of the International Zeolite Association [33]. This observation indicates that there was visible structural difference between HSOD and SSOD crystals. Strong peaks at 12° and 21° show the correct layer translation and the absence of any amorphous humps, indicating better condensation of silanol groups on adjacent layers [34, 23]. The FTIR Spectra for RUB-15 (Fig. 1.B) shows CH_3 deformation vibrations at 1488 cm^{-1} as well as asymmetric and symmetric stretching vibrations between 3000 cm^{-1} and 3200 cm^{-1}, indicating the presence of tetramethyl ammonium cations (TMA^+) [25]. In relation to the SSOD spectra the peak at 1488 cm^{-1} is absent suggesting complete removal of occluded organic matter. In addition the absence of an internally bonded OH group between 3550 cm^{-1} and 3570 cm^{-1} indicates the absence of occluded water molecules, resulting in free porous sodalite cage structures [35].

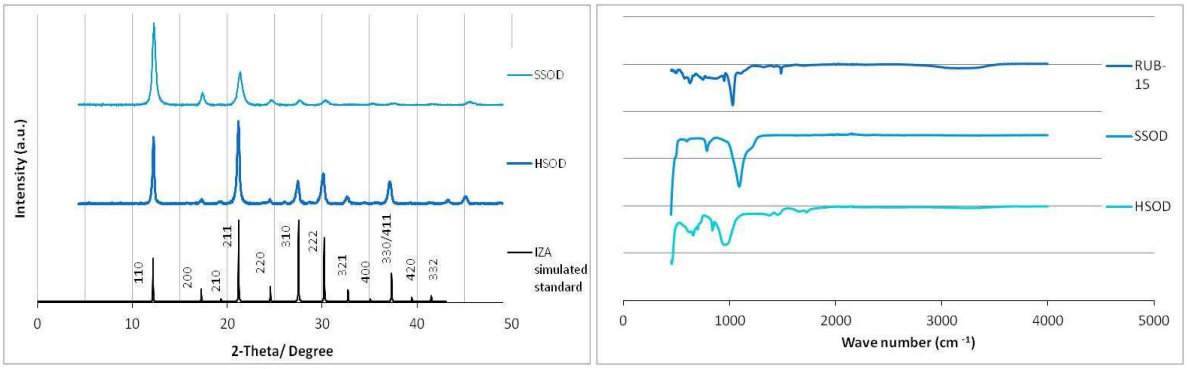

Fig. 1. A) XRD patterns for SSOD and HSOD particles compared to the simulated pattern from International Zeolite Association and B) FTIR spectra for RUB-15, SSOD and HSOD

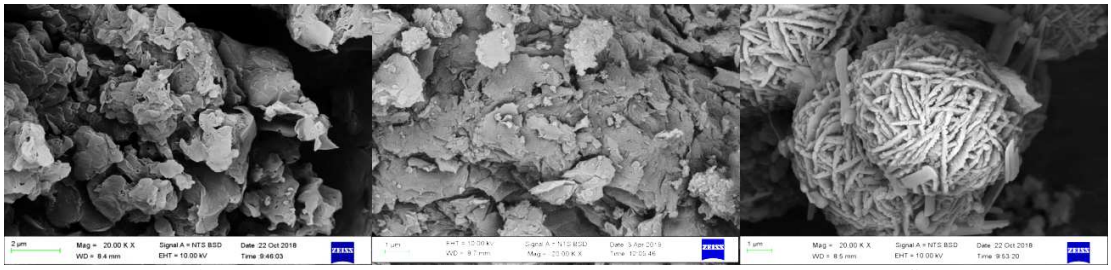

A B C

Fig. 2. SEM imaging of synthesized A) RUB-15, B) SSOD and C) HSOD (Mag= 20 000X)

SEM images of the as-produced SSOD reveal a plate like morphology of the SSOD particles similar to that of the parent RUB-15 (Fig. 2. A and B) and are in agreement with literature [36]. This suggests successful topotactic conversion of RUB-15 to SSOD through the condensation of the silanol groups on adjacent silicate layers without the breaking of layers or need for additional silicates, thereby enabling formation of structures identical to the parent layers [23]. Furthermore, the SEM image of the HSOD crystals shows the thread-ball shape similar to what has been reported in literature (see Fig. 2. C) [15, 29].

3.2. Membrane characterization

The SEM image showing the surface view and the cross-sectional view of the PSF and SSOD-infused PSF membranes are depicted in Fig. 3. The morphology of the pure PSF membranes is relatively smooth with the appearance of small surface defects formed during casting. The HSOD membranes surface shows a large amount of bubbles and striations, with small pores visible at high magnifications. Small particles just below the surface can be seen in both the HSOD and SSOD images.

The PSF membrane is asymmetric, similar to what has been reported in literature. The dense layer, as observed in the image, consists of tightly packed vertical canals of greater fractional free volume, followed by a sponge-like layer with large free voids [14, 18, 37, 38]. For the membranes, the SEM images show that SSOD and HSOD particles were dispersed within the fractional free area of the polymer with less agglomeration [26]. Increasing the SSOD loading in the membranes facilitated formation of more agglomerates within the SSOD/PSF membrane.

Tensile strength analysis of the mixed matrix membranes revealed PSF to have a high Young's modulus of 56.8 MPa, classifying the material as mechanically strong. The addition of both the HSOD and SSOD filler reduced the Young's modulus and the tensile strength of the membranes. The 5 wt. % SSOD/PSF mixed matrix membrane produced a tensile strength of 6.8 MPa which is far greater than the 2.2 and 3.27 MPa produced for asymmetric polysulfone by Tsai et al [38]. Increasing the SSOD loading resulted in an increase in Young's modulus and reduced tensile strength contrary to that expected from literature [29, 39], one possible explanation is the restriction of polymer chain movement by the increased formation of hydrogen bonds between the polymer and large agglomerates [26].

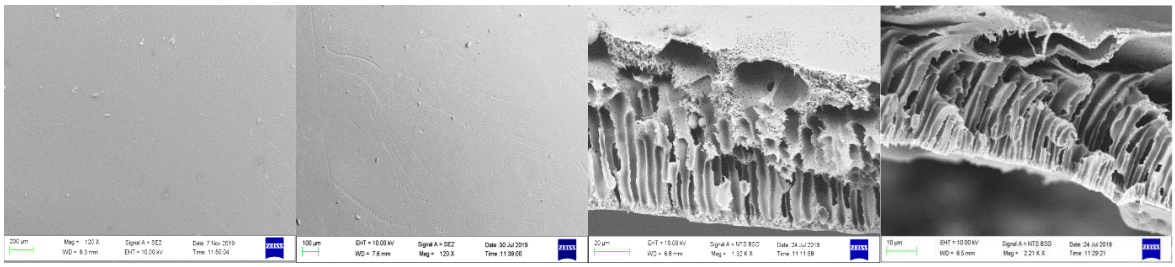

A B C D

Fig. 3. SEM surface images of A) HSOD and B) SSOD (Mag= 120 X) and cross-sectional images of C) HSOD and D) SSOD (Mag= 2 210X)

3.3. Gas separation performance

3.3.1 Effect of increased porosity sodalite on PSF membrane performance

The results of the single gas permeation and mixed gas separation of the membranes are presented in Table 1. PSF shows low permeance with high H_2/CO_2 and H_2/N_2 selectivity. The addition of SSOD positively affects the H_2 permeance of the membrane compared to PSF at the cost of reduced selectivity (5 to 1.6). The higher porosity silica sodalite had a small positive effect on membrane permeance relative to HSOD, increased selectivity of the SSOD membranes may also be attributed to the smaller pore size of the SSOD particles [26]. Common H_2/CO_2 ideal selectivity's are reported to range from 0.083 [40], 1.5- 2 [41], 2.3- 2.57 [42], 2.65- 3.17 [27] and 2.4- 4.64 [43] for zeolite/polymer composite membranes. The selectivity's reported in this study fall on the mid to lower end of this spectrum.

Under mixed gas testing ($60H_2$:$40CO_2$) the HSOD membrane outperformed both the PSF and SSOD in terms of permeance and selectivity, showing a high separation factor (SF) of 54.9 which far exceeded the Knudsen separation of 4.6 [44]. The section of SSOD membrane used in this testing may have contained greater defects and large agglomerates than seen in the representative SEM image, attributing to the increased permeance of CO_2. The permeance produce for membranes in this study exceeds that reported by Li et al at 1×10^{-8} mol/m^2.s.Pa, although higher ideal and mixed gas selectivity's were reported [28]. The HSOD H_2/CO_2 selectivity of 3.9 exceeds the ideal selectivity as well as 1.67-3.57 reported by Khan et al [45].

Table 1. Gas permeations at 1 bar_g and 25℃

Wt. %	Filler	Single Gas Testing						Mixed Gas Testing		
		Permeance ($\times10^{-9}$ mol/m^2.s.Pa)			Selectivity			Permeance ($\times10^{-7}$ mol/m^2.s.Pa)		Separation factor
		H_2	N_2	CO_2	H_2/CO_2	H_2/N_2	N_2/CO_2	H_2	CO_2	H_2/CO_2
0		2.725	1.977	1.974	5.008	4.965	1.009	4.922	4.22	2.191
5	HSOD	7.313	5.842	5.549	1.068	1.051	1.017	27.170	10.459	54.946
5	SSOD	7.751	5.992	5.768	1.604	1.513	1.060	4.970	12.431	0.573
10	SSOD	7.538	7.354	7.261	1.038	1.026	1.012	6.544	8.857	1.135
15	SSOD	7.650	7.315	7.190	1.066	1.047	1.018	9.714	19.299	0.726

3.3.2 Effect on increased silica sodalite loading on PSF membranes performance

Increasing the SSOD loading produced a parabolic increase in membrane permeability with a cap at 10 wt. % SSOD. This may be attributed to tortuosity around regions of high sodalite agglomeration which was seen at increasing sodalite loading [46]. Selectivity decreases with increased SSOD loading up to 10 wt. % after which the selectivity remains relatively constant. This is likely due to the high volume of surface defects and enhanced free volume of the membrane with increased agglomerate size at higher sodalite loading, eventually the increased loading reduces void space, pores become blocked and mass transfer resistance is increased [37].

The same parabolic cap was seen at 10 wt. % for H_2/CO_2 SF, reaching a maximum of 1.1. Membrane permeance was positively affected by increasing SSOD loading with no maximum peak.

3.3.3 Effect of increased pressure

Increasing the upstream pressure from 1 to 5 bar_g resulted in an exponential decrease in H_2 (Fig 4.A), CO_2 and N_2 permeability's in single gas permeations of all membranes except the PSF which remained relatively stable, this is a common behaviour for glassy polymers such as PSF. Increasing pressure occupied the Langmuir sorption sites in the dense layer resulting in an increased permeate pressure and reduced solubility [47]. SSOD filled membranes exhibited an improved permeability up to 2-3 bar_g under mixed gas testing followed by a reduction resulting in an overall decrease. Selectivity remained relatively constant with changes in upstream pressure, with the exception of the HSOD which exhibited a high selectivity at 1 bar_g (Fig. 4.B).

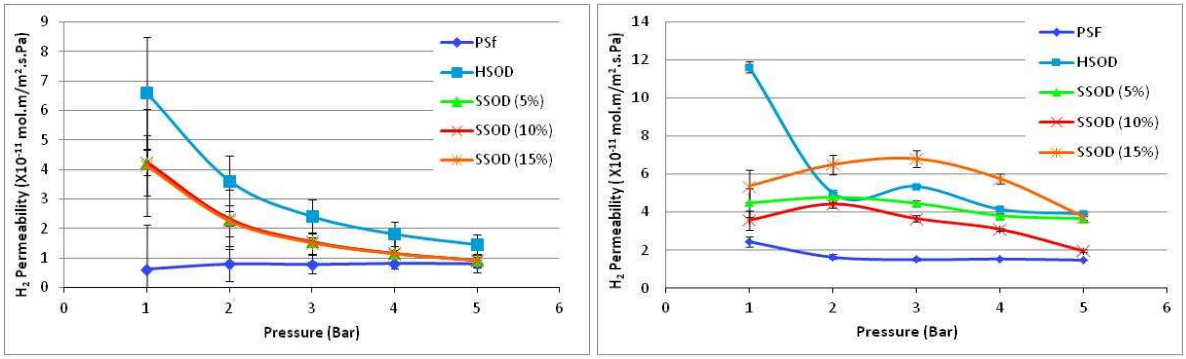

A B

Fig. 4. Hydrogen permeability vs. pressure for A) pure H_2 and B) $60H_2$:$40CO_2$ mixed gas

4. Conclusions

Mixed membranes utilizing high porosity silica sodalite have the potential for low energy intensity, low cost H_2/CO_2 separation with application in IGCC pre-combustion processes if membrane separation performance can be adequately improved. This study analysed the morphology and textural properties of silica sodalite in relation to hydrothermally produced hydroxy sodalite and found the SSOD to be of higher surface area and pore volume. The SSOD synthesized was mesoporous of a plate like morphology with slit-like pores, in relation the HSOD crystals were of spherical, thread ball morphology. Both sodalite variations displayed high crystallinity and the absence of occluded water and organic matter. The sodalite was incorporated in polysulfone mixed matrix membranes and found to have an asymmetric morphology, high mechanical strength despite surface defects produced during casting. Although the addition of SSOD to the PSF mixed matrix membranes reduced the ideal selectivity from 5 to 1.6, pure hydrogen permeance was increased from 2.7×10^{-9} to 7.8×10^{-9} mol/m^2.s.Pa. While SSOD performed within the region of selectivity reported in literature. The HSOD/PSF mixed matrix membrane displayed a high selectivity of 3.9 and permeance of 27.2×10^{-9} mol/m^2.s.Pa in mixed gas testing (60 H_2:40 CO_2). Increasing the SSOD loading was advantageous up to 10 wt.% producing a selectivity of 1.1 and permeance of 6.5×10^{-9} mol/m^2.s.Pa. Although the results are promising, membrane performance still requires some improvement for potential use in IGCC applications. A different fabrication procedure or solvent may allow for improved surface morphology and the reduction of free voids within the membrane, surface modifications or coatings could also be a viable option to produce highly permeable and selective membranes for H_2/CO_2 separation.

Acknowledgements

The authors would like to acknowledge Air Product South Africa for the funding of this research as well as the University of the Witwatersrand, School of Chemical and Metallurgical Engineering laboratory support staff for their assistance with this research.

References

[1] F. Dong, Y. Wang, B. Su, Y. Hua and Y. Zhang, The process of peak CO_2 emissions in developed economies: A perspective of industrialization and urbanization, *Resources, Conservation & Recycling,*141 (2019) pp. 61-75

[2] D. Leung, G. Caramanna and M. Mercedes Maroto-Valer, An overview of current status of carbon dioxide capture and storage technologies, *Renewable and Sustainable Energy Reviews,* 39 (2014) pp. 426-443.

[3] B. Smith, M. Loganathan and M. Shantha, A review of the water-gas shift reaction kinetics, *International journal of chemical reactor engineering,* 8, no. Review R4 (2010).

[4] N. M. Anwar, A. Fayyaz, N. F. Sohail, M. F. Khokhar, M. Khokhar, W. D. Khan, K. Rasool, M. Rehan and A. S. Nizami, CO_2 capture and storage: A way forward for sustainable environment, *Journal of Environmental*

Management, 226 (2018) pp. 131-144,.

[5] C. Gouedard, D. Picq, F. Launay and P. L. Carrette, Amine degradation in CO_2 capture I. A review, *International journal of greenhouse gas control,* 10 (2012) pp. 244-270.

[6] A. J. Reynolds, T. V. Verheyen, S. B. Adeloju, E. Meuleman and P. Feron, Towards commercial scale post-combustion capture of CO_2 with monoethanolamine solvent: Key considerations for solvent management and environmental impacts, *Environmental science and technology,* 43 (2010) pp. 3643-3654.

[7] A. Basu, J. Akhtar, M. Rahman and M. Islam, A review of separation of gasses using membrane systems," *Petroleum Science and Technology,* 22 (2004) p. 1343.

[8] C. Scholes, K. Smith, S. Kentish and G. Stevens, CO_2 capture from pre-combustion processes—Strategies for membrane gas separation, *Intarnational Journal of Greenhouse Gas Control,* 4 (2010) pp. 739-755.

[9] R. Baker, Membrane separation systems: recent developments and future directions, New Jearsey, Park Ridge, 1991.

[10] S. P. Nunes and K. Peinemann, Membrane Technology in the Chemical Industry, Weinheim, Wiley & Sons Inc., 2001.

[11] L.-J. Wang and F. C.-N. Hong, Effects of surface treatments and annealing on carbon-based molecular sieve membranes for gas separation, *Applied Surface Science,* 240, 1-4 (2005) pp. 161-174.

[12] L. M. Robeson, Correlation of separation factor versus permeability for polymetric membranes, *Journal of membrane science,* 62 (1991) p. 165.

[13] L. M. Robeson, The upper bound revisited, *Journal of membrane science,* 320 (2008) pp. 390-400.

[14] S. Madaeni and P. Moradi, Preparation and characterization of asymmetric polysulfone membrane for separation of oxygen and nitrogen gases, *Journal of applied polymer science,* 121, 4 (2011) pp. 2157-2167,

[15] M. Daramola, O. Oloye and A. Yaya, Nanocomposite sodalite/ceramic membrane for pre-combustion CO_2 capture: synthesis and morphological characterization, *International journal of coal science & technology,* 4, 1 (2017) pp. 60-66.

[16] M. O. Daramola, E. F. Aransiola and T. V. Ojumu, Potential Applications of Zeolite Membranes in Reaction Coupling Separation Processes, *Materials,* 5, 11 (2012) pp. 2101-2136.

[17] S. Chakraborty, B. Wang and P. Dutta, Tolerance of polymer-zeolite composite membranes to mechanical strain, *Journal of membrane science,* 518 (2016) pp. 192-202.

[18] J. Ahn, W.-J. Chung, I. Pinnau and M. D. Guiver, Polysulfone/silica nanoparticle mixed-matrix membranes for gas separation, *Journal of membrane science,* 314 (2008) pp. 123-133

[19] C. A. Scholes, S. E. Kentish and G. W. Stevens, Carbon Dioxide Separation through Polymeric Membrane Systems for Flue Gas Applications, *Recent Patents on Chemical Engineering,* 1 (2008) pp. 52-66.

[20] D. W. Breck, Zeolite Molecular Sieves Structure, Chemistry and Use, New York, Wiley & Sons Inc., 1974.

[21] S. Khajavi, S. Sartipi, J. Gascon, J. Jansen and F. Kapteijn, Thermostability of hydroxy sodalite in view of membrane applications, *Microporous and mesoporous materials,* 132 (2010) p. 510.

[22] M. Daramola, A. Dinat and S. Hasrod, Synthesis and Characterization of Nanocomposite Hydroxy-Sodalite/Ceramic Membrane via Pore-Plugging Hydrothermal Synthesis Technique, *Journal of Membrane and Separation Technology,* 4 (2015) pp. 1-7.

[23] T. Moteki, W. Chaikitisilp, A. Shimojima and T. Okuba, Silica sodalite without occluded organic maatter by topotactic conversion of lamellar precursor, *American Chemical Society,* 130 (2008) pp. 15780-15781.

[24] T. Moteki, W. Chaikitisilp, Y. Sakamoto, A. Shimojima and T. Okuba, Role of Acidic Pretreatment of Layered Silicate RUB-15 in its Topotactic Conversion into Pure Silica Sodalite, *Chemistry of materials,* 23 (2011) pp. 3564-3570.

[25] M. Koike, Y. Asakura, M. Sugihara, Y. Kuroda, H. Tsuzura, H. Wada, A. Shimojima and K. Kuroda, Topotactic conversion of layered silicate RUB-15 to silica sodalite through interlayer condensation in N-methylformamide, *Dalton Transactions,* 46 (2017) pp. 10232-10239

[26] D. Bastani, N. Esmaeili and M. Asadollahi, Polymeric mixed matrix membranes containing zeolites as a filler for gas separation applications: A review, *Journal of Industrial and Engineering Chemistry,* 19 (2013) pp. 375-393.

[27] A. Huang, H. Bux, F. Steinbach and J. Caro, Molecular-Sieve Membrane with Hydrogen Permselectivity: ZIF-22 in LTA Topology Prepared with 3-Aminopropyltriethoxysilane as Covalent Linker, *Angewandte Chemie,* 122, 29 (2010) pp. 2075-5081

[28] Y. Li, F. Liang, H. Bux, W. Yang and J. Caro, Zelitic imidazolate framework ZIF-7 based molecular sieve membrane for hydrogen separation, *Journal of membrane science,* 354 (2010) pp. 48-54.

[29] M. Daramola, B. Silinda, S. Masondo and O. Oluwasina, Polyethersulphone-sodalite (PES-SOD) Polyethersulphone-sodalite (PES-SOD) mixed-matrix membranes: prospects for acid mine drainage (AMD) treatment, *The South African Institute of Minning and Metallurgy,* 115 (2015) pp. 1221-1228.

[30] S. Hashemifard, A. Ismail and T. Matsuura, Mixed matrix membrane incorporated with large pore size halloysite nanotubes (HNT) as filler for gas separation: Experimental, *Journal of Colloid and Interface Science,* 359 (2011) pp. 359-370

[31] D. D. Reible and F. H. Shair, A technique for the measurement of gaseous diffusion in porous media, *Journal of soil science,* 33 (1982) pp. 165-174.

[32] P. Zhang, Adsorption and Desorption Isotherms, Ke Research Group, 2016.

[33] International Zeolite Association, Database of Zeolite Structures, http://europe.iza-structure.org/IZA-SC/framework.php?STC=SOD, 2007 (Accessed May 2019).

[34] C. L. Eden and M. O. Daramola, Development of silica sodalite with enhanced porosity via topotactic synthesis for pre-combustion CO_2 capture, in *SINTEF proceedings no.4 (*ISBN 978-82-536-1646-9), Trondheim, Norway, 2019, pp 13-20.

[35] J. Coates, Interpretation of Infrared Spectra, A Practical Approach, *Encyclopedia of Analytical Chemistry,* (2006) pp. 1-23.

[36] U. Oberhagemann, P. Bayat, B. Marler, H. Gies and J. Rius, A Layer Silicate: Synthesis and Structure of the Zeolite Precursor RUB-15—$[N(CH_3)_4]_8[Si_{24}O_{52}(OH)_4]\cdot_{20} H_2O$, *Angewandte chemie international edition,* 35, 23-24 (1996) pp. 2869-2872

[37] I. Pinnau and W. J. Koros, Structures and Gas Separation Properties of Asymmetric Polysulfone Membranes Made by Dry, Wet and Dry/ Wet Phase Inversion, *Journal of Applied Polymer Science,* 43 (1991) pp. 1491-1502.

[38] H. A. Tsai, D. H. Huang, R. C. Ruaan and J. Y. Lai, Mechanical Properties of Asymmetric Polysulfone Membranes Containing Surfactant as Additives, *Industrial and Engineering Chemistry Research,* 40, 25 (2001) pp. 5917-5922.

[39] Y. Shen and A. Lua, Preparation and characterization of mixed matrix membranes based on poly(vinylidene fluoride) and zeolite 4A for gas separation, *Polymer engineering science,* 52 (2012) pp. 2106-2113.

[40] P. Jha and J. D. Way, Carbon dioxide selective mixed-matrix membranes formulation and characterization using rubbery substituted polyphosphazene, *Journal of Membrane Science,* 324, 1-2 (2008) pp. 151-161.

[41] T. Weng, H. Tseng and M. Wey, Fabrication and characterization of poly(phenylene oxide)/SBA-15/carbon molecule sieve multilayer mixed matrix membrane for gas separation, *International journal of hydrogen energy,* 35 (2010) pp. 6971-6983.

[42] Y. Zhang, K. Balkus, I. H. Musselman and J. P. Ferraris, Mixed-matrix membranes composed of Matrimid® and mesoporous ZSM-5 nanoparticles, *Journal of Membrane Science,* 325 (2008) pp. 28-39.

[43] E. Karatay, H. Kalıpçılar and L. Yılmaz, Preparation and performance assessment of binary and ternary PES-SAPO 34-HMA based gas separation membranes, *Journal of membrane science,* 364, 1-2 (2010) pp. 75-81.

[44] M. Vaezi and A. Babaluo, Effect of dehydration temperature on the H_2 separation potential of hydroxy sodalite zeolite membranes, *Iranian Journal of Hydrogen & Fuel Cell,* 4 (2014) pp. 209-214.

[45] A. J. Khan, A. Cano-Odena, B. Gutiérrez, C. Minguillón and I. F. J. Vankelecom, Hydrogen separation and purification using polysulfone acrylate–zeolite mixed matrix membranes, *Journal of Membrane Science,* 350 (2010) pp. 340-346.

[46] S. Kim, C. Dr. Marand, S. Dr. Oyama, R. Dr. Davis and V. Dr. Guliants, *High permeability/ high diffusivity mixed matrix membranes for gas separation,* Blacksburg, Virginia: Virginia Polytechnic Insitute and State University, 2007.

[47] P. Li, T. S. Chung and D. R. Paul, Gas sorption and permeation in PIM-1, *Journal of Membrane Science,* 432 (2013) pp. 50-57.